

HFMCA: ORTHONORMAL FEATURE LEARNING FOR EEG-BASED BRAIN DECODING

Yinghao WANG¹, Lintao XU², Shujian YU³, Enzo TARTAGLIONE¹, Van-Tam NGUYEN¹

¹LTCI, Télécom Paris, Institute Polytechnique de Paris, Palaiseau, France

²LIGM, Univ Gustave Eiffel, École des Ponts, CNRS, Marne-la-Vallée, France

³Department of Artificial Intelligence, Vrije Universiteit Amsterdam, Amsterdam, The Netherlands

ABSTRACT

Electroencephalography (EEG) analysis is critical for brain-computer interfaces and neuroscience, but the intrinsic noise and high dimensionality of EEG signals hinder effective feature learning. We propose a self-supervised framework based on the Hierarchical Functional Maximal Correlation Algorithm (HFMCA), which learns orthonormal EEG representations by enforcing feature decorrelation and reducing redundancy. This design enables robust capture of essential brain dynamics for various EEG recognition tasks. We validate HFMCA on two benchmark datasets, SEED and BCIC-2A, where pretraining with HFMCA consistently outperforms competitive self-supervised baselines, achieving notable gains in classification accuracy. Across diverse EEG tasks, our method demonstrates superior cross-subject generalization under leave-one-subject-out validation, advancing state-of-the-art by 2.71% on SEED emotion recognition and 2.57% on BCIC-2A motor imagery classification. Our code and supplementary material are available at: https://github.com/W-Yinghao/HFMCA_EEG.

Index Terms— Contrastive self-supervised learning, EEG emotion recognition, EEG motor imagery

1. INTRODUCTION

Electroencephalography (EEG) offers a non-invasive window into brain activity, capturing electrical signals that reflect complex neural dynamics across multiple spatiotemporal scales. This modality is indispensable for clinical monitoring and brain-computer interfaces (BCIs), particularly in applications like emotion recognition and motor imagery tasks where physiological signals provide objective biomarkers. However, developing robust and generalizable EEG analysis systems faces significant barriers, primarily stemming from three core challenges. First, the high-dimensional spatiotemporal patterns inherent in multi-channel recordings present difficulties for direct modeling and feature extraction. Second, the analysis is complicated by the extremely low signal-to-noise ratio (SNR), which is further sharpened by substantial inter-subject variability. Third, and critically, the acquisition of large-scale,

expertly annotated EEG datasets is prohibitively expensive and time-consuming, creating a severe bottleneck that limits the application of data-hungry fully supervised deep learning approaches.

Contrastive self-supervised learning (SSL) has emerged as a powerful paradigm for leveraging unlabeled EEG data to overcome annotation scarcity. By learning to maximize agreement between differently augmented views of the same instance while minimizing similarity between distinct instances, contrastive SSL encourages the model to extract invariant and semantically meaningful features. This process inherently improves generalization by reducing reliance on spurious correlations [1] and forcing the encoder to focus on robust, biologically relevant patterns. The resulting representations demonstrate improved transferability across tasks and subjects, and enhanced robustness to inter-session and inter-subject variability, which are key challenges in EEG decoding. Furthermore, by leveraging vast amounts of unlabeled data, contrastive SSL effectively regularizes the model, leading to flatter loss landscapes and better out-of-sample performance [2]. Building on well-known frameworks like SimCLR [3] and MoCo [4], EEG-based Contrastive SSL methods typically generate positive pairs by applying diverse augmentations to the same raw EEG sample, while treating segments from different samples/trials as negatives. Recent approaches have made progress in addressing domain-specific challenges. Temporal modeling methods such as TS-TCC [5] learn robust representations via cross-view prediction, while spatial modeling approaches like CL-SSTER [6] use attention to capture inter-channel relationships. For cross-domain generalization, CLISA [7] addresses domain adaptation in EEG, and multimodal frameworks [8] exploit complementary information across modalities to enhance learning.

However, persistent limitations remain: 1) current frameworks typically decouple temporal and spatial modeling, treating them as independent dimensions rather than jointly learning their complementary representations; 2) conventional negative sampling, which typically relies on random selection across different trials or subjects, is highly prone to semantic contamination given EEG's low SNR and inter-subject variability. This may group similar brain states as negatives or fail to separate dissimilar, noise-corrupted states [9],

thereby degrading representation quality and cross-subject generalizability.

This paper presents the Hierarchical Functional Maximal Correlation Algorithm (HFMCA) for self-supervised EEG representation learning and makes three key contributions:

- We introduce HFMCA in Sec. 2.1, a hierarchical contrastive self-supervised framework that employs Functional Maximal Correlation Analysis (FMCA) [10] to maximize dependence between low-level representations (augmentations from more than two views) and the corresponding high-level fused representation [11], while enforcing orthogonality on encoder outputs. This design is fundamentally different from frameworks like SimCLR or MoCo, where the central idea is to maximize dependence between two augmented parallel views.
- We extend HFMCA to HFMCA++ in Sec. 2.2, by incorporating an additional regularization term that minimizes the similarity between the averaged low-level features of an instance and the high-level representations of other instances within a batch, which further enhances the discriminative power of the learned representations.
- Under leave-one-subject-out validation paradigm, our method demonstrates state-of-the-art cross-subject generalization on both the SEED emotion recognition benchmark and motor imagery classification task, surpassing previous best methods by 2.71% and 2.54% in mean accuracy, respectively, described in Sec. 3.

2. METHODOLOGY

Hierarchical Functional Maximal Correlation Algorithm utilizes multiview SSL to investigate the hierarchical relationships between the data and their augmentations.

2.1. Hierarchical FMCA for Self-Supervised Learning

Similar to other SSL methods, HFMCA utilizes data augmentations to learn meaningful representations. Let us consider an instance X and a set of augmentations, as described by Eq. 1, where $Y_i = T_i(X)$ and T_i signifies i -th augmentation function (e.g., temporal masking or channel dropout):

$$\mathcal{Y} = \{Y_1, Y_2, \dots, Y_T\}, \quad (1)$$

The core concept of our approach posits that each data augmentation generates a distinct low-level representation, capturing a unique perspective of the underlying instance. Aggregating all augmentation-derived low-level features yields a unified high-level representation that summarizes the multiple views and semantically captures the original instance. Specifically, we define $\hat{\rho}$ as the statistical dependence between: (1) the complete *set of low-level features* \mathcal{S} (with variability governed by distribution $P(\mathcal{S})$), and (2) their aggregated *high-level summary* \mathcal{Z} (governed by $P(\mathcal{Z})$). This dependence $\hat{\rho}$ is

defined as the density ratio between $P(\mathcal{S}, \mathcal{Z})$ and $P(\mathcal{S})P(\mathcal{Z})$, and admits an orthogonal decomposition [10, 12]:

$$\hat{\rho}(\mathcal{S}, \mathcal{Z}) = \frac{p(\mathcal{S}, \mathcal{Z})}{p(\mathcal{S})p(\mathcal{Z})} = \sum_{k=1}^{\infty} \sqrt{\sigma_k} \phi_k(\mathcal{S}) \psi_k(\mathcal{Z}). \quad (2)$$

This decomposition arises from the eigenanalysis of a cross-covariance operator between the reproducing kernel Hilbert spaces (RKHSs) of \mathcal{S} and \mathcal{Z} , where σ_k denotes the k -th eigenvalue quantifying the strength of the k -th mode of dependence between \mathcal{S} and \mathcal{Z} . The corresponding orthogonal eigenfunctions, $\phi_k(\cdot)$ and $\psi_k(\cdot)$, form complete bases in their respective RKHS, satisfying:

$$\mathbb{E}_{\mathcal{S}} [\phi_i(\mathcal{S}) \phi_j(\mathcal{S})] = \mathbb{E}_{\mathcal{Z}} [\psi_i(\mathcal{Z}) \psi_j(\mathcal{Z})] = \begin{cases} 1, & i = j \\ 0, & i \neq j \end{cases}$$

To extract hierarchical features from the augmented samples, we employ two neural networks f_{θ} and g_{ω} . Given T augmented views $\{Y_1, Y_2, \dots, Y_T\}$ generated from an input instance, we first extract low-level features using a weight-sharing encoder f_{θ} (Fig. 1). The set of low-level features \mathcal{S} and aggregated high-level representation \mathcal{Z} are obtained by:

$$\begin{aligned} \mathcal{S} &= \{S_i\}_{i=1}^T = \{f_{\theta}(Y_1), f_{\theta}(Y_2), \dots, f_{\theta}(Y_T)\} \\ \mathcal{Z} &= g_{\omega}(\text{concat}(S_1, S_2, \dots, S_T)), \end{aligned} \quad (3)$$

where $\text{concat}(\cdot)$ denotes the concatenation operation. This hierarchical feature extraction strategy allows \mathcal{Z} to integrate information across all augmentations, forming a comprehensive representation that preserves both view-specific details and global semantics.

Using the low-level feature set $\mathcal{S} = \{S_1, \dots, S_T\}$ and high-level representation \mathcal{Z} from Eq. 3, we compute the correlation matrices as Eq. 4:

$$\begin{aligned} R_1 &= \mathbb{E} \left[\frac{1}{T} \sum_{t=1}^T S_t (S_t)^{\top} \right] & R_2 &= \mathbb{E} [ZZ^{\top}] \\ P_{1,2} &= \mathbb{E} \left[\frac{1}{T} \sum_{t=1}^T S_t Z^{\top} \right] & R_{1,2} &= \begin{bmatrix} R_1 & P_{1,2} \\ P_{1,2}^{\top} & R_2 \end{bmatrix}. \end{aligned} \quad (4)$$

To maximize the statistical dependence between hierarchical features \mathcal{S} and \mathcal{Z} while promoting feature orthogonality, we minimize a loss function based on log-determinants (logdet) of the correlation matrices [13, 10]. Specifically, we:

- Minimize $\log \det R_{1,2}$ to enhance dependence between \mathcal{S} and \mathcal{Z} .
- Maximize $\log \det R_1$ and $\log \det R_2$ to encourage orthogonality within each feature set.

This yields the optimization objective shown in Eq. 5:

$$\min_{\theta, \omega} \mathcal{L}_{\text{logdet}} = \underbrace{\log \det R_{1,2}}_{\text{enhance dependence}} - \underbrace{\log \det R_1 - \log \det R_2}_{\text{promote orthogonality}}. \quad (5)$$

Minimizing this objective simultaneously strengthens the relationship between hierarchical representations while encouraging disentangled features within each level.

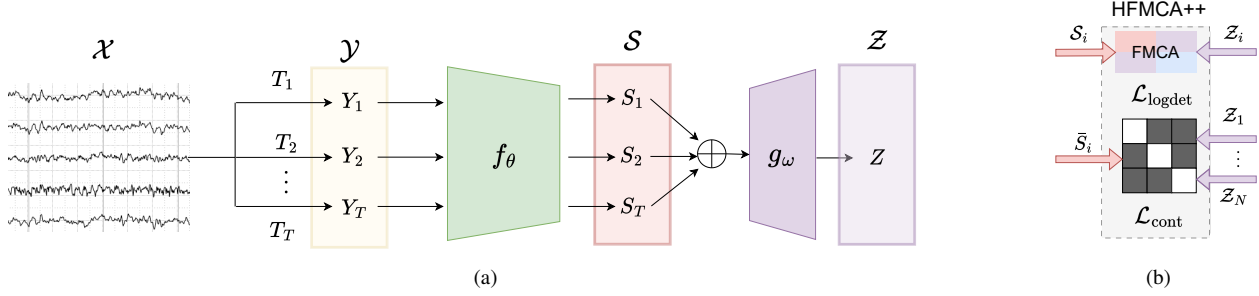


Fig. 1: (a) Architecture diagram of the HFMCA framework. The raw EEG signal \mathcal{X} is transformed by functions T_i to generate augmented inputs \mathcal{Y} . The encoder f_θ extracts low-level features \mathcal{S} , which are concatenated and fed into g_ω to produce the high-level instance representation \mathcal{Z} . (b) Loss function structure: HFMCA++ employs a hybrid loss $\mathcal{L}_{\text{HFMCA++}}$ composed of the FMCA-based density ratio loss $\mathcal{L}_{\text{logdet}}$ and the cross-instance contrastive loss $\mathcal{L}_{\text{cont}}$.

2.2. HFMCA++: Preventing Trivial Solutions via Contrastive Regularization

While HFMCA effectively models hierarchical relationships, we observe that the high-level representation \mathcal{Z} is susceptible to over-smoothing or dimensional redundancy, which can cause it to collapse to a trivial solution where all instances map to similar embeddings. To address this limitation, we extend HFMCA to HFMCA++ by incorporating an efficient contrastive regularization term. This novel component minimizes similarity between the averaged low-level features of an instance and the high-level representations of other instances within a batch. Formally, for a batch of N instances, we first compute the averaged low-level feature for the i -th instance:

$$\bar{\mathcal{S}} = \frac{1}{T} \sum_{t=1}^T \mathcal{S}_t. \quad (6)$$

The contrastive regularization term is then defined as:

$$\mathcal{L}_{\text{cont}} = \frac{1}{N(N-1)} \sum_{i=1}^N \sum_{j \neq i} \exp \left(\frac{\bar{\mathcal{S}}_i \cdot \mathcal{Z}_j}{\tau} \right), \quad (7)$$

where τ is a temperature hyperparameter controlling similarity scaling. This contrastive mechanism operates as a repulsive force in the embedding space, ensuring that the high-level representation \mathcal{Z}_i maintains discriminative information specific to instance i rather than collapsing to a constant solution. The complete HFMCA++ objective becomes:

$$\min_{\theta, \omega} \mathcal{L}_{\text{HFMCA++}} = \mathcal{L}_{\text{logdet}} + \lambda \mathcal{L}_{\text{cont}}, \quad (8)$$

with $\lambda \geq 0$ balances maximization of the dependence and the additional regularization term.

The instance-level contrastive loss in HFMCA++ inherently avoids trivial solutions through three mechanisms: (1) augmentation-invariant non-uniformity enforcement via cross-hierarchy asymmetric contrasting of averaged low-level features ($\bar{\mathcal{S}}_i$) against cross-instance high-level representations (\mathcal{Z}_j), (2) implicit dimensionality preservation from

orthogonal encoder constraints from HFMCA, and (3) cross-hierarchy regularization that filters noise while retaining discriminative variance. Crucially, compared to SimCLR’s augmentation-dependent approach, our method reduces inductive bias by leveraging natural inter-instance negatives rather than artificial augmentations. This is particularly vital for EEG data where valid transformations lack theoretical grounding.

3. EXPERIMENTS

Datasets: To evaluate the performance of our proposed method, we conducted extensive experiments on two publicly available and widely used EEG benchmark datasets:

- **BCIC-2A** [14]: contains EEG data from 9 subjects performing four different motor imagery (MI) tasks: imagination of movement of the left hand, right hand, both feet, and tongue. The recordings were acquired using 22 EEG channels at a sampling frequency of 250 Hz. Each subject consists of 72 trials per class (288 trials total). Similarly, we segmented each trial into non-overlapping 4-second segments to create the input samples. The downstream task is a four-class classification problem to identify the imagined movement.
- **SEED** [15]: comprises EEG recordings from 15 subjects collected during emotion elicitation experiments using 15 film clips, resulting in 5 trials per emotion category per subject. The data was recorded using 62 electrodes at a sampling rate of 200 Hz. For our experiments, we segmented each trial into non-overlapping 2-second epochs, resulting in multiple samples per trial for self-supervised pre-training. The final classification task was to predict the emotion label (positive, neutral, or negative) of each trial.

Data Augmentation Strategies: To learn robust representations in a self-supervised manner, we employ a diverse set of data augmentation techniques specifically de-

signed for EEG signals. Given an input EEG segment $X = (Channels, Time)$, we apply the following transformations: (1) Channel Permutation; (2) Temporal Masking; (3) Channel Dropout, and (4) Temporal Crop-and-Resize. This combination of spatial (channel-based) and temporal augmentations creates a rich set of views for each input, which is crucial for effective contrastive learning. A visualization of the different augmentations and implementation details is provided in the supplementary material.

Network Architecture: The encoder network f_θ was adopted from the architecture presented in [13] for SEED, and in [16] for BCIC-2A, which are specifically designed for effective EEG representation learning. The projection head g_ω is implemented as a 3-layer Multilayer Perceptron (MLP) with a hidden layer size of 512 and ReLU activation functions.

Evaluation Protocol: Following standard SSL practices, upon completion of the pretext training stage, we freeze the parameters of the pretrained encoder f_θ . A logistic regression (LR) classifier is subsequently trained atop these frozen representations to evaluate the learned embeddings' quality on downstream classification tasks. This protocol provides a rigorous and parameter-efficient assessment of the encoder's representational capacity, ensuring fair comparison with state-of-the-art methods.

Quantitative Analysis: Tables 1 and 2 present the experimental results on the SEED dataset and BCIC-2A dataset, respectively. Overall, HFMCA and HFMCA++ demonstrate superior performance among all compared methods, achieving the second-highest (56.43%) and highest (58.74%) average accuracy on SEED, respectively.

At the individual subject level, HFMCA++ achieves the best or second-best classification accuracy on 11 out of 15 subjects in the SEED dataset, demonstrating robust cross-subject generalization capability. The results on the BCIC IVa dataset further corroborate these findings. HFMCA++ consistently achieves the highest average accuracy and obtains the best or second-best performance across the majority of subjects. This cross-dataset consistency demonstrates that our proposed method is not only effective for emotion recognition but also generalizes well to other EEG tasks such as motor imagery classification. Such task-agnostic performance validates the robustness of the HFMCA framework.

Compared to conventional self-supervised learning methods, HFMCA achieves an improvement of approximately 4–8 percentage points, which represents a significant advancement in EEG signal analysis. This substantial performance gain can be attributed to our hierarchical feature modeling, which effectively captures both temporal dynamics and inter-channel relationships in EEG signals.

4. CONCLUSION AND FUTURE WORK

In this work, we presented HFMCA, a novel hierarchical self-supervised learning framework for EEG representa-

Table 1: Comparative results on SEED emotion recognition dataset. We report the classification accuracy (%) of our proposed HFMCA and HFMCA++ against five baseline methods, including MoCo [4], SimCLR [3], BYOL [17], SimSiam [18] and ContraWR [19]. The best results are shown in bold, while the second-best results are underlined.

Subject	MoCo	SimCLR	BYOL	SimSiam	ContraWR	HFMCA	HFMCA++
S1	40.69	44.17	42.41	41.63	48.56	<u>50.92</u>	53.54
S2	40.48	48.70	39.52	42.25	42.58	<u>48.25</u>	47.88
S3	45.96	61.99	52.19	47.84	56.45	59.38	<u>59.73</u>
S4	51.31	49.03	50.08	45.61	<u>51.29</u>	47.14	49.61
S5	47.54	50.77	<u>52.78</u>	48.07	49.13	49.91	53.15
S6	61.53	59.05	64.71	62.21	61.98	60.49	<u>62.55</u>
S7	39.27	<u>49.70</u>	44.15	51.73	46.96	49.62	49.60
S8	60.80	61.92	60.06	54.89	<u>63.58</u>	60.57	64.07
S9	57.54	58.30	59.36	56.45	58.25	56.18	<u>59.11</u>
S10	50.40	56.62	53.25	59.40	55.32	56.63	<u>58.73</u>
S11	58.54	<u>67.51</u>	64.65	61.49	66.45	67.35	71.45
S12	45.52	49.03	<u>49.66</u>	51.14	<u>49.66</u>	46.44	49.52
S13	54.03	57.66	60.20	56.21	58.46	<u>61.27</u>	64.89
S14	52.47	60.14	55.73	57.33	59.07	<u>60.30</u>	63.54
S15	56.62	66.11	60.06	64.59	57.85	<u>72.01</u>	73.74
Avg	50.84	56.03	53.92	53.39	55.04	<u>56.43</u>	58.74

Table 2: Comparative results on BCIC-2A motor imagery classification dataset.

Subject	MoCo	SimCLR	BYOL	SimSiam	ContraWR	HFMCA	HFMCA++
S1	39.58	39.75	35.94	35.24	40.10	41.49	40.97
S2	39.58	41.32	38.02	41.49	43.05	<u>43.40</u>	44.10
S3	42.36	43.58	41.67	47.05	47.74	50.86	50.69
S4	37.33	37.33	35.76	36.63	38.54	39.58	39.06
S5	39.24	47.22	43.75	43.92	47.04	52.60	52.60
S6	39.24	39.76	35.93	33.68	37.50	<u>42.36</u>	43.23
S7	42.53	48.78	43.40	43.23	50.35	<u>55.38</u>	55.56
S8	39.41	40.97	38.19	40.62	41.84	<u>44.27</u>	47.56
S9	42.88	44.27	42.53	<u>44.79</u>	45.83	40.79	41.32
Avg	40.24	42.89	38.35	40.73	43.55	<u>45.63</u>	46.12

tion learning that effectively balances feature dependence and discriminative power. By combining log-determinant minimization for hierarchical feature alignment with an efficient contrastive regularization mechanism, our approach prevents representation collapse while maintaining computational efficiency. Validation on SEED and BCIC-2A dataset demonstrates state-of-the-art performance, with HFMCA++ achieving 2.71% and 2.57% higher accuracy compared to conventional contrastive methods, respectively. The learned representations show enhanced discriminative power and improved cross-subject generalization capabilities, critical for real-world brain-computer interface applications. Future work will explore:

- Extending the hierarchical framework to incorporate temporal dynamics of EEG signals,
- Investigating domain adaptation capabilities for cross-dataset transfer learning,
- Exploring HFMCA to develop EEG foundation models by leveraging large-scale data from diverse cohorts.

5. ACKNOWLEDGEMENT

This work was supported by the French National Research Agency (ANR) in the framework of the IA Cluster project “Hi! PARIS Cluster 2030” under Grant ANR-23-IACL-005, and by the Hi! PARIS Center on Data Analytics and Artificial Intelligence.

6. REFERENCES

- [1] Michael Zhang, Nimit S Sohoni, Hongyang R Zhang, Chelsea Finn, and Christopher Re, “Correct-n-contrast: a contrastive approach for improving robustness to spurious correlations,” in *ICML*, 2022, pp. 26484–26516.
- [2] Philip Fradkin, Lazar Atanackovic, and Michael R Zhang, “Robustness to adversarial gradients: A glimpse into the loss landscape of contrastive pre-training,” in *ICML Workshop*, 2022.
- [3] Ting Chen, Simon Kornblith, Mohammad Norouzi, and Geoffrey Hinton, “A simple framework for contrastive learning of visual representations,” in *International conference on machine learning*, 2020, pp. 1597–1607.
- [4] Kaiming He, Haoqi Fan, Yuxin Wu, Saining Xie, and Ross Girshick, “Momentum contrast for unsupervised visual representation learning,” in *CVPR*, 2020, pp. 9729–9738.
- [5] Emadeldeen Eldele et al., “Self-supervised contrastive representation learning for semi-supervised time-series classification,” *IEEE Transactions on Pattern Analysis and Machine Intelligence*, vol. 45, no. 12, pp. 15604–15618, 2023.
- [6] Xinke Shen, Lingyi Tao, Xuyang Chen, Sen Song, Quanying Liu, and Dan Zhang, “Contrastive learning of shared spatiotemporal eeg representations across individuals for naturalistic neuroscience,” *NeuroImage*, vol. 301, pp. 120890, 2024.
- [7] Xinke Shen, Xianggen Liu, Xin Hu, Dan Zhang, and Sen Song, “Contrastive learning of subject-invariant eeg representations for cross-subject emotion recognition,” *IEEE Transactions on Affective Computing*, vol. 14, no. 3, pp. 2496–2511, 2022.
- [8] Qi Fan, Yutong Li, Yi Xin, Xinyu Cheng, Guanglai Gao, and Miao Ma, “Leveraging contrastive learning and self-training for multimodal emotion recognition with limited labeled samples,” in *Proceedings of the 2nd International Workshop on Multimodal and Responsible Affective Computing*, 2024, pp. 72–77.
- [9] Haoning Kan, Jiale Yu, Jiajin Huang, Zihe Liu, Heqian Wang, and Haiyan Zhou, “Self-supervised group meiosis contrastive learning for eeg-based emotion recognition,” *Applied Intelligence*, vol. 53, no. 22, pp. 27207–27225, 2023.
- [10] Bo Hu and Jose C Principe, “The normalized cross density functional: A framework to quantify statistical dependence for random processes,” *arXiv preprint arXiv:2212.04631*, 2022.
- [11] Bo Hu, Yuheng Bu, and José C Príncipe, “Learning orthonormal features in self-supervised learning using functional maximal correlation,” in *IEEE International Conference on Image Processing*, 2024, pp. 472–478.
- [12] Shao-Lun Huang, Anuran Makur, Gregory W Worrell, and Lihong Zheng, “Universal features for high-dimensional learning and inference,” *Foundations and Trends® in Communications and Information Theory*, vol. 21, no. 1-2, pp. 1–299, 2024.
- [13] Shihan Ma, Bo Hu, Tianyu Jia, Alexander Clarke, Blanka Zicher, Arnault Caillet, Dario Farina, and José C Príncipe, “Learning cortico-muscular dependence through orthonormal decomposition of density ratios,” *NeurIPS*, vol. 37, pp. 129303–129328, 2024.
- [14] Michael Tangermann et al., “Review of the bci competition iv,” *Frontiers in neuroscience*, vol. 6, pp. 55, 2012.
- [15] Wei-Long Zheng and Bao-Liang Lu, “Investigating critical frequency bands and channels for eeg-based emotion recognition with deep neural networks,” *IEEE Transactions on autonomous mental development*, vol. 7, no. 3, pp. 162–175, 2015.
- [16] Wenjie Li, Haoyu Li, Xinlin Sun, Huicong Kang, Shan An, Guoxin Wang, and Zhongke Gao, “Self-supervised contrastive learning for eeg-based cross-subject motor imagery recognition,” *Journal of Neural Engineering*, vol. 21, no. 2, pp. 026038, 2024.
- [17] Jean-Bastien Grill et al., “Bootstrap your own latent—a new approach to self-supervised learning,” *Advances in neural information processing systems*, vol. 33, pp. 21271–21284, 2020.
- [18] Xinlei Chen and Kaiming He, “Exploring simple siamese representation learning,” in *Proceedings of the IEEE/CVF conference on computer vision and pattern recognition*, 2021, pp. 15750–15758.
- [19] Chaoqi Yang, Cao Xiao, M Brandon Westover, and Jimeng Sun, “Self-supervised electroencephalogram representation learning for automatic sleep staging: model development and evaluation study,” *JMIR AI*, vol. 2, no. 1, pp. e46769, 2023.